HHS Public Access

Author manuscript

Sci Transl Med. Author manuscript; available in PMC 2018 January 18.

Published in final edited form as:

Sci Transl Med. 2017 January 18; 9(373): . doi:10.1126/scitranslmed.aai8030.

Tyrosine kinase blocking collagen IV–derived peptide suppresses ocular neovascularization and vascular leakage

Raquel Lima e Silva[#1,2], **Yogita Kanan**[#1,2], **Adam C. Mirando**[3], **Jayoung Kim**[3,4], **Ron B. Shmueli**[3,4], **Valeria E. Lorenc**[1,2], **Seth D. Fortmann**[1,2], **Jason Sciamanna**[1,2], **Niranjan B. Pandey**[3,5], **Jordan J. Green**[1,3,4,6], **Aleksander S. Popel**[3], and **Peter A. Campochiaro**[1,2,†]

[1]Department of Ophthalmology, Johns Hopkins University School of Medicine, Baltimore, MD 21205, USA

[2]Department of Neuroscience, Johns Hopkins University School of Medicine, Baltimore, MD 21205, USA

[3]Department of Biomedical Engineering, Johns Hopkins University School of Medicine, Baltimore, MD 21205, USA

[4]Translational Tissue Engineering Center, Johns Hopkins University School of Medicine, Baltimore, MD 21205, USA

[5]AsclepiX Therapeutics, LLC, Baltimore, MD 21211, USA

[6]Institute for Nanobiotechnology, Johns Hopkins University School of Medicine, Baltimore, MD 21205, USA

[#] These authors contributed equally to this work.

[†]Corresponding author. pcampo@jhmi.edu.

Author contributions: R.L.e.S. assisted in experimental design, performed experiments, collected and interpreted data, prepared the figures, assisted in writing Materials and Methods and legends, and edited and approved the manuscript. Y.K. assisted in experimental design; performed experiments; collected and interpreted data; prepared the figures; assisted in writing Materials and Methods, legends, and Results; and edited and approved the manuscript. A.C.M. assisted in experimental design, performed experiments, collected and interpreted data, prepared the figures, assisted in writing Materials and Methods and legends, and edited and approved the manuscript. J.K. assisted in experimental design, performed experiments, and collected and interpreted data. R.B.S. assisted in experimental design, performed experiments, collected and interpreted data, and edited and approved the manuscript. V.E.L. assisted in experimental design, performed experiments, collected and interpreted data, and edited and approved the manuscript. S.D.F. assisted in experimental design, performed experiments, collected and interpreted data, and edited and approved the manuscript. J.S. performed experiments, collected data, and edited and approved the manuscript. N.B.P. assisted in experimental design, supervised experimental work, interpreted data, assisted in troubleshooting, edited and approved the manuscript, and provided funding. J.J.G. assisted in experimental design, supervised experimental work, interpreted data, assisted in troubleshooting, edited and approved the manuscript, and provided funding. A.S.P. assisted in experimental design, supervised experimental work, interpreted data, assisted in troubleshooting, edited and approved the manuscript, and provided funding. P.A.C. assisted in experimental design, supervised experimental work, interpreted data, assisted in troubleshooting, wrote the first draft of the manuscript, and provided funding.

Competing interests: J.J.G. and A.S.P. are the cofounders and serve as the chief technology officer and chief science officer, and N.B.P. is the senior director of research and development of AsclepiX Therapeutics, LLC. P.A.C. is a consultant for AsclepiX Therapeutics, LLC, and several competing companies: Aerpio Therapeutics, Alimera, Applied Genetic Technologies, Genentech/Roche, Graybug, Regeneron, Allegro, Intrexon, and Regenxbio. The Johns Hopkins University receives research funding on behalf of P.A.C. from AbbVie, Alimera, Allergan, Aerpio Therapeutics, Genentech/Roche, Genzyme, GlaxoSmithKline, Oxford Biomedica, and Regeneron. The terms of these arrangements are being managed by the Johns Hopkins University in accordance with its conflict of interest policies.

Data and materials availability: Complete data are available from the corresponding author upon request.

Abstract

Vascular endothelial growth factor (VEGF)–neutralizing proteins provide benefit in several retinal and choroidal vascular diseases, but some patients still experience suboptimal outcomes, and the need for frequent intraocular injections is a barrier to good outcomes. A mimetic peptide derived from collagen IV, AXT107, suppressed subretinal neovascularization (NV) in two mouse models predictive of effects in neovascular age-related macular degeneration (NVAMD) and inhibited retinal NV in a model predictive of effects in ischemic retinopathies. A combination of AXT107 and the current treatment aflibercept suppressed subretinal NV better than either agent alone. Furthermore, AXT107 caused regression of choroidal NV. AXT107 reduced the VEGF-induced vascular leakage that underlies macular edema in ischemic retinopathies and NVAMD. In rabbit eyes, which are closer to the size of human eyes, intraocular injection of AXT107 significantly reduced VEGF-induced vascular leakage by 86% at 1 month and 70% at 2 months; aflibercept significantly reduced leakage by 69% at 1 month and did not reduce leakage at 2 months, demonstrating the longer effectiveness of AXT107. AXT107 reduced ligand-induced phosphorylation of multiple receptors: VEGFR2, c-Met, and PDGFRβ. Optimal signaling through these receptors requires complex formation with β_3 integrin, which was reduced by AXT107 binding to $\alpha_v\beta_3$. AXT107 also reduced total VEGFR2 levels by increasing internalization, ubiquitination, and degradation. This biomimetic peptide is a sustained, multitargeted therapy that may provide advantages over intraocular injections of specific VEGF-neutralizing proteins.

INTRODUCTION

Neovascularization (NV) is a critical component of wound repair that must be precisely controlled: the process must be initiated quickly to replace damaged vasculature and terminated just as quickly when revascularization is complete. Control is achieved by balancing proangiogenic proteins that stimulate the process with antiangiogenic proteins that slow it down. Proteolysis of extracellular matrix facilitates growth of new vessels throughout avascular tissue but, through an elegant adaptation, also helps to slow the process by cleaving various proteins into antiangiogenic fragments including angiostatin, endostatin, and collagen IV peptides (*1*–*3*). Because such protein fragments are physiologic angiogenesis inhibitors, they are appealing candidates for treatment of pathologic angiogenesis; however, attempts to use them as therapeutics have been unsuccessful. Despite formation by proteolytic cleavage, these proteins are still quite large and provide challenges with regard to manufacturing, maintaining appropriate folding and/or stability, and penetrating into tissues. One strategy to overcome these issues is to identify the sequences within these proteins responsible for their antiangiogenic activity and use them as a starting point to design mimetic peptides that are more potent and more easily delivered to target tissues. Using methods of systems biology, numerous peptide sequences with potential antiangiogenic activity have been identified and the corresponding peptides have been synthesized and tested in endothelial cell proliferation and migration assays (*4*). Peptides with substantial activity in vitro were tested in animal models of pathologic NV (*5*–*10*). A family of peptides derived from collagen IV showed substantial antiangiogenic activity (*11*). As reported in this study, we generated, through structure-activity studies and modification

to facilitate synthesis, a 20-mer peptide, AXT107, with structure LRRFSTAPFAFI-DINDVINF.

Neovascular age-related macular degeneration (NVAMD), diabetic retinopathy, and retinal vein occlusions are prevalent causes of visual disability in which NV and excessive vascular leakage are critical pathologic processes and hence targets for therapeutic intervention. There are good animal models for these diseases, which are ideal for testing the antiangiogenic and antipermeability activity of drugs and biologics and for investigating their molecular mechanism (*12*). Here, we also investigated the effects of AXT107 in these models.

RESULTS

AXT107 suppresses and regresses choroidal NV

The outer retina is normally completely avascular and receives oxygen and nutrients from choroidal vessels by diffusion/transport through the retinal pigmented epithelium (RPE). In choroidal NV, new vessels grow from the choroid into the sub-RPE and subretinal spaces, disrupting the outer blood-retinal barrier and resulting in collection of fluid within the retina and loss of vision. The most prevalent disease process in which this occurs is NVAMD, but it also occurs in diseases in which Bruch's membrane and the RPE are compromised. Mice in which Bruch's membrane and the RPE are ruptured by laser photocoagulation provide a model of choroidal NV in which testing of anti– vascular endothelial growth factor (VEGF) agents has been predictive of outcomes in clinical trials (*13–15*). Using these mice, we compared the mean area of choroidal NV at Bruch's membrane rupture sites in eyes injected with 1 mg of scrambled control peptide to the mean area of choroidal NV in eyes injected with 1 μg of AXT107 and found that the AXT107-treated eyes showed significantly less NV, comparable to that seen in eyes injected with 40 μg of aflibercept (Fig. 1A). Injection of 0.1 μg of AXT107 had no significant effect. Compared to injection of 1 μg of AXT107 or 40 μg of aflibercept, injection of the combination was superior, causing significantly greater reduction of choroidal NV area (Fig. 1B). To determine the effect of AXT107 on established NV, we did not treat a large cohort of mice for 7 days after rupture of Bruch's membrane, at which point the baseline area of NV was measured in a subgroup of mice (Fig. 1C, baseline) and the remainder had intraocular injection of 0.1 or 1 μg of AXT107 or 1 μg of control peptide. At day 14, the area of choroidal NV in eyes injected with 1 μg, but not 0.1 μg, of AXT107 was significantly less than the baseline area, indicating regression of the choroidal NV, even after establishment of pathology (Fig. 1C).

AXT107 suppresses subretinal NV in rho/VEGF mice

Transgenic mice in which the rhodopsin promoter drives expression of VEGF in photoreceptors (*rho/VEGF* mice) develop buds of NV that originate from the deep capillary bed of the retina and grow into the subretinal space (*16, 17*). This type of NV occurs in about 30% of patients with NVAMD and is referred to as retinal angiomatous proliferation or type 3 choroidal NV (*18*). Intraocular injection of 1 μg of AXT107 at postnatal day (P) 14 caused a significant reduction in the mean area of this type of subretinal NV at P21 when compared with controls (Fig. 2A).

AXT107 suppresses ischemia-induced retinal NV

Mice with oxygen-induced ischemic retinopathy (OIR) are exposed to high levels of oxygen at P7, causing regression of newly formed retinal vessels and areas of nonperfusion (*19*). When returned to room air at P12, the poorly perfused retina is hypoxic, resulting in high expression of VEGF and other hypoxia-regulated gene products and causing retinal NV at P17 (*20*). This model is most analogous to retinopathy of prematurity but is also relevant to proliferative diabetic retinopathy. Intraocular injection of 1 μg, but not 0.1 μg, of AXT107 at P12 caused a significant reduction in the area of retina NV per retina in mice with OIR (Fig. 2B).

AXT107 suppresses VEGF-induced leakage

Rho/VEGF mice were given an intraocular injection of vehicle or 1 μg of AXT107 at P20 after subretinal NV had developed. At P21, leakage of serum albumin from the NV was significantly reduced in AXT107-injected eyes compared with controls (Fig. 3A). *Tet/opsin/VEGF* double-transgenic mice express high levels of VEGF in the retina when treated with doxycycline, resulting in severe vascular leakage. Within 4 days, these mice develop exudative retinal detachment in a high percentage of eyes (*21*). In six mice given an intraocular injection of 1 μg of AXT107 at the onset of doxycycline treatment, five had no detachment, one developed a partial detachment, and there were no total detachments after 4 days of doxycycline (Fig. 3, B and C). In six mice given an intraocular injection of 40 μg of aflibercept, one developed a total detachment, one developed a partial detachment, and four mice had no detachment. All six control mice treated with vehicle developed total retinal detachments 4 days after initiation of doxycycline, significantly more than in the AXT107 or aflibercept groups (Fig. 3C).

Mouse models provide useful tests of biologic activity, but the small size of the eye makes it difficult to predict doses and duration of activity for human eyes, which are much larger. A rabbit eye more closely approximates the size of a human eye, and although the distribution of retinal vessels differs from that of a human eye, they respond to VEGF with prominent leakage similar to primate and human eyes (*22*). AXT107 (50 μg) was injected into the inferior part of the vitreous in one eye of Dutch Belted rabbits. Fundus photographs taken 2 days later showed a clear vitreous cavity with no sign of inflammation (similar to the uninjected, fellow control eye) and a gel-like depot presumed to be the peptide in the inferior vitreous at the site of injection (Fig. 4A, left panel, arrows). The gel-like depot was still present in the same location 30 days after injection (third panel, arrows). In preliminary experiments, we found that intraocular injection of 10 μg of VEGF caused profuse leakage of intravascularly injected sodium fluorescein into the vitreous of Dutch Belted rabbits. With vitreous fluorophotometry (VFP), we precisely measured the fluorescein that leaked from the retinal vessels into the vitreous cavity and showed that peak leakage occurred 7 days after intraocular injection of 10 μg of VEGF and returned to baseline over the subsequent 7 days. Three days after injection of 50 μg of AXT107 in one eye, 10 μg of VEGF was injected in both eyes, and 7 days later, VFP showed that fluorescein leakage was reduced by 60% in AXT107-injected eyes compared with control fellow eyes (Fig. 4B). In another group of rabbits, the effect of AXT107 was compared to that of aflibercept. Twenty-three days after injection of 50 μg of AXT107 or 500 μg of aflibercept (this is equivalent to the

clinical dose because the rabbit vitreous is one-fifth of that in humans) in one eye, 10 μg of VEGF was injected into both eyes. Representative VFP scans obtained on day 30 show the concentration of fluorescein along the visual axis of the eye, and the mid-vitreous concentration of fluorescein (area under the curve between 5 and 7 mm in front of the retina) was lower in AXT107- and aflibercept-injected eyes than in fellow eye controls (Fig. 4C). The mid-vitreous fluorescein concentration provides an assessment of retinal vascular leakage and was reduced from that in fellow eye controls by 86% in AXT107-injected eyes and 69% in aflibercept-injected eyes (Fig. 4D). Thirteen days later, on day 43, the rabbits were rescanned without injection of fluorescein, and vitreous fluorescence was back to baseline. The rabbits were rechallenged by intraocular injection of 10 μg of VEGF on day 53; representative scans obtained on day 60 show low levels of fluorescein in the mid-vitreous of AXT107-injected eyes, but we did not observe similar inhibition in control or aflibercept-injected eyes (Fig. 4E). Compared with fellow eye controls, leakage was reduced by 70% by AXT107, but was not significantly reduced by aflibercept (Fig. 4F), demonstrating the superiority of AXT107 at reducing leakage over time.

AXT107 binds $\alpha_5\beta_1$ and $\alpha_v\beta_3$ integrins

We have previously demonstrated that the parent peptide to AXT107 disrupts antibody-epitope interactions between α_1 and $\alpha_v\beta_3$ integrins and their respective antibodies, implicating the integrin heterodimers $\alpha_x\beta_1$ and $\alpha_v\beta_3$ as targets for the peptide (*4*). Human retinal endothelial cells (HRECs) show immunohistochemical staining with antibodies specific for the α_5 integrin monomer or the $\alpha_v\beta_3$ integrin heterodimer, which is reduced by preincubation with 50 μM AXT107 and eliminated by preincubation with 100 or 200 μM AXT107 (Fig. 5A). To directly test for and quantify binding of AXT107 to $\alpha_5\beta_1$ and $\alpha_v\beta_3$, we monitored the changes in fluorescence anisotropy of 5-carboxyfluorescein (5-FAM)–labeled AXT107 that had been incubated with a range of concentrations of recombinant $\alpha_v\beta_3$ or $\alpha_5\beta_1$. The binding isotherms showed high-affinity binding of AXT107 to integrin $\alpha_v\beta_3$ (Fig. 5B) and integrin $\alpha_5\beta_1$ (Fig. 5C), with dissociation constant (K_d) values of 1.29 and 2.21 nM, respectively.

AXT107 suppresses phosphorylation of VEGFR2, c-Met, and PDGFRβ

Integrin $\alpha_v\beta_3$ forms complexes with VEGF receptor 2 (VEGFR2) and platelet-derived growth factor receptor β (PDGFRβ) that enhance ligand-induced phosphorylation and downstream signaling (*23–25*). Therefore, we tested the effect of AXT107 on VEGF-induced phosphorylation of VEGFR2 in HRECs and PDGF-BB–induced phosphorylation of PDGFRβ in mouse 3T3 fibroblasts. We also tested the effect of hepatocyte growth factor (HGF)–induced phosphorylation of c-Met. Incubation of HRECs with VEGF (25 ng/ml) for 5 min resulted in optimal phosphorylation of VEGFR2, whereas incubation with HGF (50 ng/ml) for 15 min resulted in optimal phosphorylation of c-Met. Incubation of 3T3 cells with PDGF-BB (50 ng/ml) for 5 min resulted in optimal phosphorylation of PDGFRβ. HRECs were preincubated with increasing concentrations of AXT107 for 90 min before addition of VEGF (25 ng/ml) for 5 min or HGF (50 ng/ml) for 15 min; VEGF-induced phosphorylation of VEGFR2 and HGF-induced phosphorylation of c-Met were reduced by 25 μM AXT107 and further reduced by 50 or 100 μM AXT107 (Fig. 6,A and B). Concentrations of 50 or 100 μM AXT107 also reduced total VEGFR2 and c-Met. The AXT107-induced reduction in

phosphorylation of VEGFR2 and c-Met began at lower doses and was greater than the reduction in the respective receptor proteins. In 3T3 cells, concentrations of AXT107 (≥10 μM) reduced phosphorylation of PDGFRb (Fig. 6C).

$\alpha_v\beta_3$ integrin is important for activation of VEGFR2, as shown by its increased association in the presence of VEGF, which increases downstream signaling events, and because treatment with an anti-β_3 antibody suppresses VEGF-induced phosphorylation of VEGFR2 (*23*). We therefore investigated the effect of AXT107 on VEGFR2-β_3 complex formation. HRECs were incubated with VEGF (25 ng/ml) in the presence or absence of 60 μM AXT107s. Cell lysates were immunoprecipitated with anti-VEGFR2 and immunoblotted with anti-VEGFR2 and anti-β_3. Compared to the immunoprecipitate from cells stimulated with VEGF in the absence of AXT107, the immunoprecipitate from cells stimulated with VEGF in the presence of AXT107 showed slightly less VEGFR2 and a large reduction in β_3 integrin. This indicates that AXT107 disrupts VEGFR2-β_3 complex formation, a critical step for VEGFR2 signaling (Fig. 6D).

In addition, VEGF signaling is further reduced by the AXT107-induced reduction of VEGFR2 protein levels. To investigate whether this is a result of ubiquitin-mediated degradation [as occurs with prolonged stimulation with VEGF (*26*)], we exposed HRECs to three conditions (no stimulation, stimulation with VEGF, and stimulation with VEGF in the presence of 60 μM AXT107) and immunoblotted cell lysates with anti–phospho-VEGFR2 and anti-VEGFR2. AXT107 caused a 53% reduction in total VEGFR2 (Fig. 6E, left). To compensate for the 53% reduction in VEGFR2, we used twice as much lysate from cells treated with VEGF in the presence of AXT107 (than from cells stimulated with VEGF in the absence of AXT107) for immunoprecipitation with anti-VEGFR2. The immunoprecipitates were immunoblotted with the anti-ubiquitin antibody FK2, and the blot was reprobed with anti-VEGFR2. We detected a band for ubiquitinated VEGFR2 in immunoprecipitates from VEGF-stimulated HRECs incubated with 60 μM AXT107 (Fig. 6, arrowhead) but not in immunoprecipitates from VEGF-stimulated HRECs in the absence of peptide, although there were equal amounts of VEGFR2. Furthermore, inhibition of the proteasome by lactacystin reduced AXT107-induced degradation of VEGFR2 (Fig. 6F). On average, cells treated with 100 μM AXT107 exhibited 1.4 times more total VEGFR2 in the presence of lactacystin than in control conditions. These data support the hypothesis that AXT107 promotes VEGFR2 degradation in the proteasome.

DISCUSSION

Pathologic angiogenesis or excessive vascular leakage (or both) occurs in several retinal/choroidal vascular diseases. Choroidal NV occurs in AMD, the most common cause of moderate and severe vision loss in patients over the age of 60 years (*27*). Diabetic retinopathy is a common cause of vision loss in working age patients; vision loss can occur from retinal NV, leading to vitreous hemorrhage and retinal detachment, or from excess vascular leakage resulting in macular edema (*27*). Retinal NV and macular edema also cause vision loss in patients with retinal vein occlusion. This group of highly prevalent diseases shares molecular mechanisms because, in each, stabilization of hypoxia-inducible factor–1α (HIF-1α) plays an important role (*28*–*32*). Stabilization of HIF-1α causes increased

production of several hypoxia-regulated vaso-active proteins that contribute to NV and vascular leakage (*12*). VEGF plays a particularly important role, and intraocular injections of VEGF-neutralizing proteins provide substantial benefits in NVAMD (*15, 33*), diabetic macular edema (DME) (*34, 35*), macular edema due to retinal vein occlusions (*36–38*), and background diabetic retinopathy (*39*).

Although progress has been encouraging, there is still considerable unmet need, particularly in NVAMD and DME in which substantial percentages of patients have a suboptimal response to suppression of VEGF, probably because other hypoxia-regulated vasoactive proteins participate in disease in those patients. Also, many patients with NVAMD who respond well initially to VEGF suppression ultimately lose the benefits they attained as a result of the development of subretinal fibrosis and/or macular atrophy (*40*). Similarly, patients with DME or macular edema from retinal vein occlusion who show marked improvement in vision during a period of frequent injections of a VEGF-neutralizing protein often lose much of these initial gains during periods of less frequent injections; ultimately, they experience permanent reduction in vision (*41–43*). In clinical practice, the frequency of injections is substantially less than that in clinical trials, and visual outcomes are much worse (*44*). Thus, treatments that target other hypoxia-regulated vasoactive proteins in addition to VEGF and that last longer than injections of VEGF-neutralizing proteins are needed.

Here, we have shown that the biomimetic optimized peptide derived from collagen IV AXT107 suppresses and causes regression of choroidal NV (which corresponds to type 2 choroidal NV in patients with NVAMD), inhibits growth of subretinal NV in rho/VEGF mice (which corresponds to type 3 choroidal NV), and reduces leakage from subretinal new vessels (the cause of macular fluid collection and acute, reversible loss of vision in NVAMD). AXT107 also inhibits ischemia-induced retinal NV, the primary pathologic process in proliferative diabetic retinopathy or proliferative complications of retinal vein occlusions, and suppresses VEGF-induced leakage from pre-existent retinal vessels, a key pathologic process in DME and macular edema due to vein occlusions. In rabbit eyes, which more closely approximate the size of human eyes, VEGF-induced vascular leakage studies investigating intraocular injections of AXT107 and aflibercept show superiority of AXT107 at 60 days (30% leakage remaining with 50 μg of AXT107 versus 100% leakage with 500 μg of aflibercept, $P < 0.05$). After intraocular injection, AXT107 forms a small gel-like depot in the inferior vitreous remote from the visual axis that slowly dissipates over months, which may be the basis for its prolonged antipermeability activity.

AXT107 reduces VEGF-induced phosphorylation of VEGFR2 at low doses and, at higher doses, enhances degradation of VEGFR2. Thus, AXT107 perturbs VEGF signaling and suppresses ocular NV and vascular leakage by two mechanisms. AXT107 also reduces ligand-induced phosphorylation of c-Met and PDGFRβ, which may also contribute. Combined neutralization of VEGF and PDGF-BB results in significantly greater suppression of murine choroidal NV and regression of choroidal NV with superior vision outcomes in patients with NVAMD than suppression of VEGF alone (*45–47*). Because AXT107 inhibits both VEGFR2 and PDGFRβ signaling and causes regression of choroidal NV, similar

superior outcomes in NVAMD as those seen with combination therapy might be expected with injection of a single small peptide.

HGF may also contribute to edema in patients with retinal vein occlusion or DME who have a suboptimal response to suppression of VEGF (*48, 49*). Inhibition of c-Met signaling by AXT107 may provide benefit in such recalcitrant patients with macular edema. VEGFR2 and PDGFRβ require complex formation with β_3 integrin for optimal ligand-induced phosphorylation and downstream signaling (*23–25*). Binding of AXT107 to $\alpha_v\beta_3$ reduces β_3-VEGFR2 complex formation, which is one mechanism by which AXT107 reduces VEGFR2 signaling in HRECs. A second mechanism is that AXT107 increases internalization of VEGFR2, ubiquitin binding, and degradation in the proteasome. We do not yet know whether AXT107 binding to $\alpha_5\beta_1$ plays any role in its antiangiogenic and antipermeability actions, but because neutralization of $\alpha_5\beta_1$ suppresses retinal and choroidal NV (*50*), this is worth future investigation.

Mice deficient in PDGF-BB during retinal vascular development show poor recruitment of pericytes to developing retinal vessels, resulting in a phenotype similar to diabetic retinopathy (*51, 52*). In adult animals, however, drugs that block both VEGF and PDGF receptors do not have any deleterious effects on retinal vessels (*53*). A clinical trial in patients with DME, in which an oral tyrosine kinase inhibitor that blocks VEGF and PDGF receptors and some isoforms of protein kinase C was tested, showed that the drug caused improvement in DME with no deleterious effects on diabetic retinopathy (*54*). Therefore, we do not anticipate problems treating DME with AXT107.

In conclusion, we combined bioinformatics to identify candidates and laboratory testing to select and optimize synthesized peptides and identified the biomimetic peptide AXT107. This newly described agent has a distinct mechanism of action: It disrupts VEGF, HGF, and PDGF-BB signaling, each of which are important in several prevalent retinal/choroidal vascular diseases. AXT107 has robust efficacy in seven experimental paradigms in models of these retinal/choroidal vascular diseases in two species (suppression of laser-induced choroidal NV in mice, regression of laser-induced choroidal NV in mice, suppression of VEGF-induced subretinal NV in mice, suppression of ischemia-induced retinal NV in mice, reduction of vascular leakage from subretinal NV in *rho/VEGF* mice, prevention of exudative retinal detachment in *Tet/opsin/VEGF* mice that express high levels of VEGF in photoreceptors, and reduction of VEGF-induced leakage in rabbits). We demonstrated superiority of AXT107 (50 μg) over aflibercept (500 μg) in rabbits at 60 days after treatment, and the combination of AXT107 (1 μg) and aflibercept (40 μg) was superior to aflibercept alone in mice with choroidal NV. Like current anti-VEGF agents, AXT107 is delivered by intravitreous injection; however, it forms a reversible in situ gel depot outside the visual axis that likely prolongs its residence time in the vitreous, which may reduce the frequency of intraocular injections needed in patients. In addition, as a relatively small peptide, AXT107 is amenable to stable, long-term, controlled release formulations, such as incorporation into polymers for sustained delivery. Although detailed safety studies using Good Laboratory Practice (GLP) have not yet been done and are needed for further development, non-GLP safety studies at an independent Clinical Research Organization demonstrated that after intravitreous injection of AXT107 in rabbits, there was no increase

in intraocular pressure, no degradation of the ocular media in the visual axis, and no retinal toxicity. Thus, AXT107 is a promising new therapeutic agent that may have advantages over current treatments for NVAMD and DME.

MATERIALS AND METHODS

Mouse model of laser-induced choroidal NV

Mice were treated in accordance with the Association for Research in Vision and Ophthalmology guidelines on the care and use of animals in research. Laser photocoagulation–induced rupture of Bruch's membrane was used to generate choroidal NV as previously described (*13*). Briefly, 4- to 5-week-old female C57BL/6 mice were anesthetized, pupils were dilated with 1% tropicamide (Alcon Laboratories Inc.), and Bruch's membrane was ruptured at 9, 12, and 3 o'clock positions of the posterior pole with a 532-nm diode laser photocoagulation (75-μm spot size, 0.1-s duration, 120 mW) using the slit lamp delivery system of an OcuLight GL Photocoagulator (Iridex) and a handheld cover slide as a contact lens. Mice then had intraocular injection of 0.1 or 1 μg of AXT107, 1 μg of scrambled control peptide, or 40 μg of aflibercept, a VEGF-neutralizing protein, which is standard care for patients with NVAMD (*14, 15*). After 7 days, mice were euthanized, and retinas were dissected, stained with FITC-conjugated GSA (Vector Laboratories), and flat-mounted. Flat mounts were examined by fluorescence microscopy, and the area of each choroidal NV was measured by image analysis with Image-Pro Plus software (Media Cybernetics) by an observer masked with respect to experimental groups. To investigate the effect of AXT107 on established choroidal NV, intraocular injections of AXT107 or control peptide were done 7 days after rupture of Bruch's membrane, and the area of choroidal NV was measured 7 days later.

Transgenic mice with VEGF expression in photoreceptors

Transgenic mice in which the *rhodopsin* promoter drives expression of VEGF in photoreceptors (*rho/VEGF* mice) have increased levels of VEGF starting at P7 and develop multiple areas of subretinal NV by P21 (*16, 17*). At P14, *rho/VEGF* mice were given an intraocular injection of 0.1 or 1 μg of AXT107 or 1 μg of control peptide. At P21, mice were euthanized, and retinas were dissected and stained with GSA. Retinal flat mounts with photoreceptors facing up were examined by fluorescence microscopy, and the area of subretinal NV was measured by image analysis by a masked observer. The effect of AXT107 on leakage from subretinal NV was measured by immunofluorescence staining for albumin of retina from PBS-perfused *rho/VEGF* mice as previously described (*55, 56*). Briefly, *rho/VEGF* mice were given an intraocular injection of 1 μg of AXT107 or vehicle at P20 and, after 24 hours, were perfused through the left ventricle with PBS. Retinas were dissected and fixed in 10% formalin for 4 hours, washed three times in PBS, and incubated in 8% normal donkey serum for 40 min at 22°C. After washing, retinas were incubated overnight in rabbit anti-mouse albumin (Abcam) in 1% Triton at 22°C. After the retinas were washed three times in PBS/1% Triton, they were incubated in Cy3-conjugated donkey anti-rabbit antibody (Jackson ImmunoResearch Laboratories Inc.) for 50 min at 22°C. Retinas were counterstained with GSA to label NV, flat-mounted, and examined by

fluorescence microscopy. The area of albumin staining per retina was measured by image analysis by a masked observer.

Mice with OIR

OIR was produced by placing litters of C57BL/6 mice in 75 ± 3% oxygen at P7 and returning them to room air at P12 when they were given an intraocular injection of 0.1 or 1 μg of AXT107 or 1 μg of control peptide. At P17, mice were euthanized, eyes were fixed in 10% phosphate-buffered formalin for 4 hours at 22°C, and retinas were dissected. After incubation in FITC-labeled GSA for 45 min, retinas were flat-mounted and examined by fluorescence microscopy. Photographs were obtained at ×5 magnification and merged into a single image to show the entire retina using the photomerge option of Photoshop CS5.4. An observer masked with respect to treatment group measured the area of NV per retina by image analysis.

Tet/opsin/VEGF double-transgenic mice

Tet/opsin/VEGF double-transgenic mice express high levels of VEGF in photoreceptors when treated with doxycycline, resulting in severe vascular leakage and exudative retinal detachments within 4 to 5 days (*21*). *Tet/opsin/VEGF* mice were given an intraocular injection of 1 μg of AXT107, 40 μg of aflibercept, or vehicle in one eye, and after 3 days, they were given drinking water containing doxycycline (2 mg/ml). On the fourth day after initiation of doxycycline, mice were anesthetized, pupils were dilated, and fundus photographs (Micron III Retinal Imaging Microscope, Phoenix Research Laboratories Inc.) and spectral domain OCT (Bioptigen Envisu R2200) were done. After imaging, mice were euthanized and 10-μm serial sections were cut through each eye. Every 10th section was stained with Mayer's hematoxylin (Sigma-Aldrich) and Eosin-Y (Richard-Allan Scientific). On the basis of the imaging and serial sections, it was determined whether eyes had total, partial, or no retinal detachment.

VEGF-induced leakage in rabbit eyes

Dutch Belted rabbits were anesthetized with an intramuscular injection of ketamine (25 mg/kg) and xylazine (2.5 mg/kg), and pupils were dilated with 2.5% phenylephrine. The conjunctiva was cleaned with 5% povidone-iodine, and an intravitreous injection of 50 μg of AXT107 or 500 μg of aflibercept was given in one eye and vehicle was injected in the other eye. Fundus photographs were done 2 and 30 days after injection. Three days after injection, 10 μg of VEGF was injected in each eye, and 7 days later, VFP was done with a Fluorotron Master ocular fluorophotometer fitted with an animal adapter (OcuMetrics). Sodium fluorescein (15 mg; AK-Fluor 10%, Akorn) was injected into an ear vein, and after 1 hour, fluorescence was measured along the visual axis from the retina to the cornea. The area under the fluorescein concentration curve between 5 and 7 mm in front of the retina was calculated. In another group of rabbits, 10 μg of VEGF was injected in both eyes 23 days after injection of 50 μg of AXT107 or 500 μg of aflibercept in one eye, and at 30 days, VFP was done. The rabbits were rescanned without injection of sodium fluorescein on day 43, and VFP was back to baseline levels. On day 53, 10 μg of VEGF was injected in each eye, and VFP was done on day 60.

Assessment of effect of AXT107 on anti-$\alpha_v\beta_3$ and anti-α_5 binding

HRECs (Lonza) were grown to confluence in eight-well chamber slides (Nunc Inc.). The cells were fixed with 4% paraformaldehyde for 20 min, followed by three PBS washes and incubation with 0, 50, 100, and 200 μM AXT107 for 1 hour. After this step, 2 μg of anti-$\alpha_v\beta_3$ or anti-α_5 antibodies (R&D Systems) was added for 1 hour. The binding of anti-$\alpha_v\beta_3$ or anti-α_5 antibodies to HRECs cells was visualized using Alexa Fluor 488–labeled secondary antibodies (Thermo Fisher Scientific).

Fluorescence anisotropy

FAM-AXT107 (10 nM) was dissolved in dimethyl sulfoxide (DMSO) and mixed with 0 to 75 nM soluble, recombinant $\alpha_5\beta_1$ and $\alpha_v\beta_3$ heterodimeric integrins (R&D Systems) in binding buffer [50 mM tris (pH 7.5), 1 mM $CaCl_2$, 1 mM $MgCl_2$, and 100 mM NaCl]. The final concentration of the DMSO vehicle was 0.0005% for all samples. The reactions were incubated on ice for at least 30 min before reading to allow binding to reach equilibrium. Changes in fluorescence anisotropy were measured with the Tecan Safire II microplate reader using vertically polarized light at 470 nm and detecting both vertically and horizontally polarized light at 540 nm. The data were plotted using GraphPad Prism version 5.0 software and fit to the following equation (Eq. 1) for ligand concentration–dependent anisotropy accounting for receptor depletion:

$$r = r_f + (r_b - r_f)\left(\frac{(K_d + [L] + [R]) - \sqrt{(-[L] - K_d - [R])^2 - 4[L][R]}}{2[L]}\right) \quad (1)$$

where r is the calculated anisotropy, [L] is the concentration of FAM-AXT107, [R] is the concentration of integrin, and r_f, r_b, and K_d are the best-fit values for the anisotropy of free FAM-AXT107, anisotropy of integrin-bound FAM-AXT107, and the equilibrium K_d of the integrin and FAM-AXT107 interaction, respectively.

Western blotting

HRECs and 3T3 fibroblasts were cultured in six-well plates overnight at 37°C in EGM-2 or Dulbecco's modified Eagle's medium, D-glucose 4.5 g/liter) (Corning) with 10% fetal bovine serum, and penicillin/streptomycin (100 U/ml; 3T3 fibroblasts). After reaching confluence, cells were serum-starved overnight in Opti-MEM I Reduced Serum Media (Thermo Fisher Scientific) and treated with the indicated concentrations of AXT107 or an equivalent amount of DMSO vehicle for 90 min. Excess DMSO was added to bring the final concentration to 0.25% (the amount present in 100 μM AXT107). Cells were then stimulated with either VEGF (25 ng/ml; R&D Systems) for 5 min, HGF (50 ng/ml; PeproTech) for 15 min, or PDGF-BB (50 ng/ml; Cell Signaling) for 10 min; washed twice with cold PBS containing calcium and magnesium; and lysed by scraping in 100 μl of cell lysis buffer (HRECs; Cell Signaling) or Blue Loading Buffer (3T3 fibroblasts; Cell Signaling) with

phosphatase inhibitors and protease inhibitors (Roche). Lysates were then sonicated and centrifuged at 9200*g* for 5 min, and the supernatants were boiled and stored at −20°C until used. Lysates were resolved by 10% SDS–polyacrylamide gel electrophoresis and transferred to polyvinylidene difluoride (PVDF) membranes for Western blot analysis. Membranes were probed with primary antibodies against phospho-VEGFR2 (Y1175), VEGFR2, phospho-Met (Y1234/Y1235), Met, phospho-PDGFRβ (Y751), PDGFRb, actin, and GAPDH (1:1000; Cell Signaling). Secondary antibodies were donkey anti-rabbit (1:10,000) and sheep anti-mouse (1:10,000).

Immunoprecipitation

After incubation in AXT107 or control medium and VEGF stimulation as described above, HRECs were lysed in 1× Cell Lysis buffer (#9803, Cell Signaling Technology). About 700 mg of total protein was immunoprecipitated with anti-VEGFR2 conjugated to Sepharose beads (Cell Signaling) overnight. Immunoprecipitates were eluted, electrophoresed, transferred to PVDF membranes, and immunoblotted with antiubiquitin antibody (1:500; Enzo) and anti-VEGFR2 antibody (1:1000, Cell Signaling). To assess VEGFR2-γ_3 complex formation, crosslinking was done before cell lysis and immunoprecipitation by incubation in 0.4% paraformaldehyde for 10 min followed by ice-cold 1.25 M glycine for 3 min (57). Immunoprecipitates were immunoblotted with anti-γ_3 antibody (1:1000, Cell Signaling).

Statistics

In experiments in which a single experimental group was compared to a single control group, statistical comparisons were made by unpaired Student's *t* test. In experiments in which multiple experimental groups were compared to a control group or there were comparisons among multiple experimental groups, comparisons were made by ANOVA Bonferroni correction for multiple comparisons. For comparison of the two dichotomous variables with the small numbers, a Fisher's exact test was used.

Acknowledgments

Funding: This work was supported by a grant from the Edward N. and Della L. Thome Memorial Foundation (Cambridge, MA); NIH NEI grants R21EY022986, R21EY026148, 1R43EY024495, and 1R43EY025903; Maryland Biotechnology Award and TEDCO Maryland Innovation Initiative Phases 1 and 3; and the Johns Hopkins-Coulter Translational Partnership.

REFERENCES AND NOTES

1. O'Reilly MS, Holmgren S, Shing Y, Chen C, Rosenthal RA, Moses M, Lane WS, Cao Y, Sage EH, Folkman J. Angiostatin: A novel angiogenesis inhibitor that mediates the suppression of metastases by a Lewis lung carcinoma. Cell. 1994; 79:315–328. [PubMed: 7525077]
2. O'Reilly MS, Boehm T, Shing Y, Fukai N, Vasios G, Lane WS, Flynn E, Birknead JR, Olsen BR, Folkman J. Endostatin: An endogenous inhibitor of angiogenesis and tumor growth. Cell. 1997; 88:277–285. [PubMed: 9008168]
3. Maeshima Y, Colorado PC, Torre A, Holthaus KA, Grankemeyer JA, Ericksen MB, Hopfer H, Xiao Y, Stillman IE, Kalluri R. Distinct antitumor properties of a type IV collagen domain derived from basement membrane. J. Biol. Chem. 2000; 275:21340–21348. [PubMed: 10766752]
4. Karagiannis ED, Popel AS. A systematic methodology for proteome-wide identification of peptides inhibiting the proliferation and migration of endothelial cells. Proc. Natl. Acad. Sci. U.S.A. 2008; 105:13775–13780. [PubMed: 18780781]

5. Shmueli RB, Ohnaka M, Miki A, Pandey NB, Lima e Silva R, Koskimaki JE, Kim J, Popel AS, Campochiaro PA, Green JJ. Long-term suppression of ocular neovascularization by intraocular injection of biodegradable polymeric particles containing a serpin-derived peptide. Biomaterials. 2013; 34:7544–7551. [PubMed: 23849876]
6. Koskimaki JE, Karagiannis ED, Rosca EV, Vesuna F, Winnard PJ Jr. Raman V, Bhujwalla ZM, Popel AS. Peptides derived from type IV collagen, CXC chemokines, and thrombospondin-1 domain-containing proteins inhibit neovascularization and suppress tumor growth in MDA-MB-231 breast cancer xenografts. Neoplasia. 2009; 11:1285–1291. [PubMed: 20019836]
7. Koskimaki JE, Karagiannis ED, Tang BC, Hammers H, Watkins DN, Pili R, Popel AS. Pentastin-1, a collagen IV derived 20-mer peptide, suppresses tumor growth in a small cell lung cancer xenograft model. BMC Cancer. 2010; 10:29. [PubMed: 20122172]
8. Rosca EV, Lai B, Koskimaki JE, Popel AS, Laterra J. Collagen IV and CXC chemokine-derived antiangiogenic peptides suppress glioma xenograft growth. Anticancer Drugs. 2012; 23:706–712. [PubMed: 22495619]
9. Rosca EV, Penet M-F, Mori N, Koskimaki JE, Lee E, Pandey NB, Bhujwalla ZM, Popel AS. A biomimetic collagen derived peptide exhibits anti-angiogenic activity in triple negative breast cancer. PLOS ONE. 2014; 9:e111901. [PubMed: 25384034]
10. Lee E, Lee SJ, Koskimaki JE, Han Z, Pandey NB, Popel AS. Inhibition of breast cancer growth and metastasis by a biomimetic peptide. Sci. Rep. 2014; 4:7139. [PubMed: 25409905]
11. Rosca EV, Koskimaki JE, Pandy NB, Tamiz AP, Popel AS. Structure-activity relationship study of collagen-derived anti-angiogenic biomimetic peptides. Chem. Biol. Drug Des. 2012; 80:27–37. [PubMed: 22405100]
12. Campochiaro PA. Molecular pathogenesis of retinal and choroidal vascular diseases. Prog. Retin. Eye Res. 2015; 49:67–81. [PubMed: 26113211]
13. Tobe T, Ortega S, Luna JD, Ozaki H, Okamoto N, Derevjanik NL, Vinores SA, Basilico C, Campochiaro PA. Targeted disruption of the FGF_2 gene does not prevent choroidal neovascularization in a murine model. Am. J. Pathol. 1998; 153:1641–1646. [PubMed: 9811357]
14. Saishin Y, Saishin Y, Takahashi K, Lima e Silva R, Hylton D, Rudge JS, Wiegand SJ, Campochiaro PA. VEGF-$TRAP_{R1R2}$ suppresses choroidal neovascularization and VEGF-induced breakdown of the blood-retinal barrier. J. Cell. Physiol. 2003; 195:241–248. [PubMed: 12652651]
15. Heier JS, Brown DM, Chong V, Korobelnik J-F, Kaiser PK, Nguyen QD, Kirchhof B, Ho A, Ogura Y, Yancopoulos GD, Stahl N, Vitti R, Berliner AJ, Soo Y, Anderesi M, Groetzbach G, Sommerauer B, Sandbrink R, Simader C, Schmidt-Erfurth U, VIEW 1 and VIEW 2 Study Groups. Intravitreal Aflibercept (VEGF Trap-Eye) in wet age-related macular degeneration. Ophthalmology. 2012; 119:2537–2548. [PubMed: 23084240]
16. Okamoto N, Tobe T, Hackett SF, Ozaki H, Vinores MA, LaRochelle W, Zack DJ, Campochiaro PA. Transgenic mice with increased expression of vascular endothelial growth factor in the retina: A new model of intraretinal and subretinal neovascularization. Am. J. Pathol. 1997; 151:281–291. [PubMed: 9212753]
17. Tobe T, Okamoto N, Vinores MA, Derevjanik NL, Vinores SA, Zack DJ, Campochiaro PA. Evolution of neovascularization in mice with overexpression of vascular endothelial growth factor in photoreceptors. Invest. Ophthalmol. Vis. Sci. 1998; 39:180–188. [PubMed: 9430560]
18. Yannuzzi LA, Negrão S, Iida T, Carvalho C, Rodriguez-Coleman H, Slakter J, Freund KB, Sorenson J, Orlock D, Borodoker N. Retinal angiomatous proliferation in age-related macular degeneration. Retina. 2001; 21:416–434. [PubMed: 11642370]
19. Smith LE, Wesolowski E, McLellan A, Kostyk SK, D'Amato R, Sullivan R, D'Amore PA. Oxygen-induced retinopathy in the mouse. Invest. Ophthalmol. Vis. Sci. 1994; 35:101–111. [PubMed: 7507904]
20. Pierce EA, Avery RL, Foley ED, Aiello LP, Smith LEH. Vascular endothelial growth factor/vascular permeability factor expression in a mouse model of retinal neovascularization. Proc. Natl. Acad. Sci. U.S.A. 1995; 92:905–909. [PubMed: 7846076]
21. Ohno-Matsui K, Hirose A, Yamamoto S, Saikia J, Okamoto N, Gehlbach P, Duh EJ, Hackett S, Chang M, Bok D, Zack DJ, Campochiaro PA. Inducible expression of vascular endothelial growth

factor in adult mice causes severe proliferative retinopathy and retinal detachment. Am. J. Pathol. 2002; 160:711–719. [PubMed: 11839592]

22. Ozaki H, Hayashi H, Vinores SA, Moromizato Y, Campochiaro PA, Oshima K. Intravitreal sustained release of VEGF causes retinal neovascularization in rabbits and breakdown of the blood–retinal barrier in rabbits and primates. Exp. Eye Res. 1997; 64:505–517. [PubMed: 9227268]
23. Soldi R, Mitola S, Strasly S, Defilippi P, Tarone G, Bussolino F. Role of $\alpha_v\beta_3$ integrin in the activation of vascular endothelial growth factor receptor-2. EMBO J. 1999; 18:882–892. [PubMed: 10022831]
24. Borges E, Jan Y, Ruoslahti E. Platelet-derived growth factor receptor β and vascular endothelial growth factor receptor 2 bind to the b_3 integrin through its extracellular domain. J. Biol. Chem. 2000; 275:39867–39873. [PubMed: 10964931]
25. Mahabeleshwar GH, Feng W, Phillips DR, Byzova TV. Integrin signaling is critical for pathological angiogenesis. J. Exp. Med. 2006; 203:2495–2507. [PubMed: 17030947]
26. Meyer RD, Srinivasan S, Singh AJ, Mahoney JE, Gharahassanlou KR, Rahimi N. PEST motif serine and tyrosine phosphorylation controls vascular endothelial growth factor receptor 2 stability and downregulation. Mol. Cell. Biol. 2011; 31:2010–2025. [PubMed: 21402774]
27. Klein, R., Klein, B. Vision disorders in diabetes. In: National Diabetes Data Group. , editor. Diabetes in America. 2. National Institutes of Health; 1995. p. 293-330.
28. Ozaki H, Yu AY, Della N, Ozaki K, Luna JD, Yamada H, Hackett SF, Okamoto N, Zack DJ, Semenza GL, Campochiaro PA. Hypoxia inducible factor-1a is increased in ischemic retina: Temporal and spatial correlation with VEGF expression. Invest. Ophthalmol. Vis. Sci. 1999; 40:182–189. [PubMed: 9888442]
29. Kelly BD, Hackett SF, Hirota K, Oshima Y, Cai Z, Berg-Dixon S, Rowan A, Yan Z, Campochiaro PA, Semenza GL. Cell type–specific regulation of angiogenic growth factor gene expression and induction of angiogenesis in nonischemic tissue by a constitutively active form of hypoxia-inducible factor 1. Circ. Res. 2003; 93:1074–1081. [PubMed: 14576200]
30. Vinores SA, Xiao W-H, Aslam S, Shen J, Oshima Y, Nambu H, Liu H, Carmeliet P, Campochiaro PA. Implication of the hypoxia response element of the VEGF promoter in mouse models of retinal and choroidal neovascularization, but not retinal vascular development. J. Cell. Physiol. 2006; 206:749–758. [PubMed: 16245301]
31. Yoshida T, Zhang H, Iwase T, Shen J, Semenza GL, Campochiaro PA. Digoxin inhibits retinal ischemia-induced HIF-1a expression and ocular neovascularization. FASEB J. 2010; 24:1759–1767. [PubMed: 20065104]
32. Iwase T, Fu J, Yoshida T, Muramatusu D, Miki A, Hashida N, Lu L, Oveson B, Lime e Silva R, Seidel C, Yang M, Connelly S, Shen J, Han B, Wu M, Semenza GL, Hanes J, Campochiaro PA. Sustained delivery of a HIF-1 antagonist for ocular neovascularization. J. Control. Release. 2013; 172:625–633. [PubMed: 24126220]
33. Rosenfeld PJ, Brown DM, Heier JS, Boyer DS, Kaiser PK, Chung CY, Kim RY, MARINA Study Group. Ranibizumab for neovascular age-related macular degeneration. N. Eng. J. Med. 2006; 355:1419–1431.
34. Nguyen QD, Tatlipinar S, Shah SM, Haller JA, Quinlan E, Sung J, Zimmer-Galler I, Do DV, Campochiaro PA. Vascular endothelial growth factor is a critical stimulus for diabetic macular edema. Am. J. Ophthalmol. 2006; 142:961–969. e4. [PubMed: 17046701]
35. Nguyen QD, Brown DM, Marcus DM, Boyer DS, Patel S, Feiner L, Gibson A, Sy J, Rundle AC, Hopkins JJ, Rubio RG, Ehrlich JS, RISE and RIDE Study Group. Ranibizumab for diabetic macular edema. Results from 2 phase III randomized trials: RISE and RIDE. Ophthalmology. 2012; 119:789–801. [PubMed: 22330964]
36. Campochiaro PA, Hafiz G, Shah SM, Nguyen QD, Ying H, Do DV, Quinlan E, Zimmer-Galler I, Haller JA, Solomon SD, Sung JU, Hadi Y, Janjua KA, Jawed N, Choy DF, Arron JR. Ranibizumab for macular edema due to retinal vein occlusions: Implication of VEGF as a critical stimulator. Mol. Ther. 2008; 16:791–799. [PubMed: 18362932]
37. Campochiaro PA, Heier JS, Feiner L, Gray S, Saroj N, Rundle AC, Murahashi WY, Rubio RG, BRAVO Investigators. Ranibizumab for macular edema following branch retinal vein occlusion:

Six-month primary end point results of a phase III study. Ophthalmology. 2010; 117:1102–1112. e1. [PubMed: 20398941]

38. Brown DM, Campochiaro PA, Singh RP, Li Z, Gray S, Saroj N, Rundle AC, Rubio RG, Murahashi WY, CRUISE Investigators. Ranibizumab for macular edema following central retinal vein occlusion: Six-month primary end point results of a phase III study. Ophthalmology. 2010; 117:1124–1133. e1. [PubMed: 20381871]
39. Ip MS, Domalpally A, Hopkins JJ, Wong P, Ehrlich JS. Long-term effects of ranibizumab on diabetic retinopathy severity and progression. Arch. Ophthalmol. 2012; 130:1145–1152. [PubMed: 22965590]
40. Comparison of Age-related Macular Degeneration Treatments Trials (CATT) Research Group. Maguire MG, Martin DF, Ying G.-s. Jaffe GJ, Daniel E, Grunwald JE, Toth CA, Ferris FL III, Fine SL. Five-year outcomes with anti–vascular endothelial growth factor treatment of neovascular age-related macular degeneration. The comparison of age-related macular degeneration treatment trials. Ophthalmology. 2016; 123:1751–1761. [PubMed: 27156698]
41. Do DV, Nguyen QD, Khwaja AA, Channa R, Sepah YJ, Sophie R, Hafiz G, Campochiaro PA, READ-2 Study Group. Ranibizumab for edema of the macula in diabetes study: 3-year outcomes and the need for prolonged frequent treatment. JAMA Ophthalmol. 2013; 131:139–145. [PubMed: 23544200]
42. Channa R, Sophie R, Khwaja AA, Do DV, Hafiz G, Nguyen QD, Campochiaro PA, READ-2 Study Group. Factors affecting visual outcomes in patients with diabetic macular edema treated with ranibizumab. Eye. 2014; 28:269–278. [PubMed: 24263379]
43. Sophie R, Hafiz G, Scott AW, Zimmer-Galler I, Nguyen QD, Ying H, Do DV, Solomon S, Sodhi A, Gehlbach P, Duh E, Baranano D, Campochiaro PA. Long term outcomes in ranibizumab-treated patients with retinal vein occlusion; the role of progression of retinal nonperfusion. Am. J. Ophthalmol. 2013; 156:693–705. e11. [PubMed: 24053892]
44. Holz FG, Tadayoni R, Beatty S, Berger A, Cereda MG, Cortez R, Hoyng CB, Hykin P, Staurenghi G, Heldner S, Bogumil T, Heah T, Sivaprad S. Multi-country real-life experience of anti-vascular endothelial growth factor therapy for wet age-related macular degeneration. Br. J. Ophthalmol. 2015; 99:220–226. [PubMed: 25193672]
45. Jo N, Mailhos C, Ju M, Cheung E, Bradley J, Nishijima K, Robinson GS, Adamis AP, Shima DT. Inhibition of platelet-derived growth factor B signaling enhances the efficacy of anti-vascular endothelial growth factor therapy in multiple models of ocular neovascularization. Am. J. Pathol. 2006; 168:2036–2053. [PubMed: 16723717]
46. Dong A, Seidel C, Snell D, Ekawardhani S, Ahlskog JKJ, Baumann M, Shen J, Iwase T, Tian J, Stevens R, Hackett SF, Stumpp MT, Campochiaro PA. Antagonism of PDGF-BB suppresses subretinal neovascularization and enhances the effects of blocking VEGF-A. Angiogenesis. 2014; 17:553–562. [PubMed: 24154861]
47. Jaffe GJ, Eliott D, Well JA, Prenner JL, Papp A, Patel S. A phase 1 study of intravitreous E10030 in combination with ranibizumab in neovascular age-related macular degeneration. Ophthalmology. 2016; 123:78–85. [PubMed: 26499921]
48. Campochiaro PA, Hafiz G, Mir TA, Scott AW, Sophie R, Shah SM, Ying HS, Lu L, Chen C, Campbell JP, Kherani S, Zimmer-Galler I, Wenick A, Han I, Paulus Y, Sodhi A, Wang G, Qian J. Pro-permeability factors after dexamethasone implant in retinal vein occlusion; the Ozurdex for retinal vein occlusion (ORVO) study. Am. J. Ophthalmol. 2015; 160:313–321. e19. [PubMed: 25908486]
49. Campochiaro PA, Hafiz G, Mir TA, Scott AW, Zimmer-Galler I, Shah SM, Wenick AS, Brady CJ, Han I, He L, Channa R, Poon D, Meyerle C, Aronow MB, Sodhi A, Handa JT, Kherani S, Han Y, Sophie R, Wang G, Qian J. Pro-permeability factors in diabetic macular edema; the diabetic macular edema treated with Ozurdex trial. Am. J. Ophthalmol. 2016; 168:13–23. [PubMed: 27130369]
50. Umeda N, Kachi S, Akiyama H, Zahn G, Vossmeyer D, Stragies R, Campochiaro PA. Suppression and regression of choroidal neovascularization by systemic administration of an $\alpha_5\beta_1$ integrin antagonist. Mol. Pharmacol. 2006; 69:1820–1828. [PubMed: 16527907]
51. Lindahl P, Johansson BR, Levéen P, Betsholtz C. Pericyte loss and microaneurysm formation in PDGF-B-deficient mice. Science. 1997; 277:242–245. [PubMed: 9211853]

52. Enge M, Bjarnegård M, Gerhardt H, Gustafsson E, Kalén M, Asker N, Hammes H-P, Shani M, Fässler R, Betsholtz C. Endothelium-specific platelet-derived growth factor-B ablation mimics diabetic retinopathy. EMBO J. 2002; 21:4307–4316. [PubMed: 12169633]

53. Miki A, Miki K, Ueno S, Wesinger DMB, Berlinicke C, Shaw GC, Usui S, Wang Y, Zack DJ, Campochiaro PA. Prolonged blockade of VEGF receptors does not damage retinal photoreceptors or ganglion cells. J. Cell. Physiol. 2010; 224:262–272. [PubMed: 20232317]

54. Campochiaro PA, C99-PKC412-003 Study Group. Reduction of diabetic macular edema by oral administration of the kinase inhibitor PKC412. Invest. Ophthalmol. Vis. Sci. 2004; 45:922–931. [PubMed: 14985312]

55. Lima e Silva R, Shen J, Gong YY, Seidel CP, Hackett SF, Kesavan K, Jacoby DB, Campochiaro PA. Agents that bind annexin A2 suppress ocular neovascularization. J. Cell. Physiol. 2010; 225:855–864. [PubMed: 20607799]

56. Shen J, Frye M, Lee BL, Reinardy JL, McClung JM, Ding K, Kojima M, Xia H, Seidel C, Lime e Silva R, Dong A, Hackett SF, Wang J, Howard BW, Vestweber D, Kontos CD, Peters KG, Campochiaro PA. Targeting VE-PTP activates TIE2 and stabilizes the ocular vasculature. J. Clin. Invest. 2014; 124:4564–4576. [PubMed: 25180601]

57. Klockenbusch C, Kast J. Optimization of formaldehyde cross-linking for protein interaction analysis of non-tagged integrin β1. J. Biomed. Biotechnol. 2010; 2010:927585. [PubMed: 20634879]

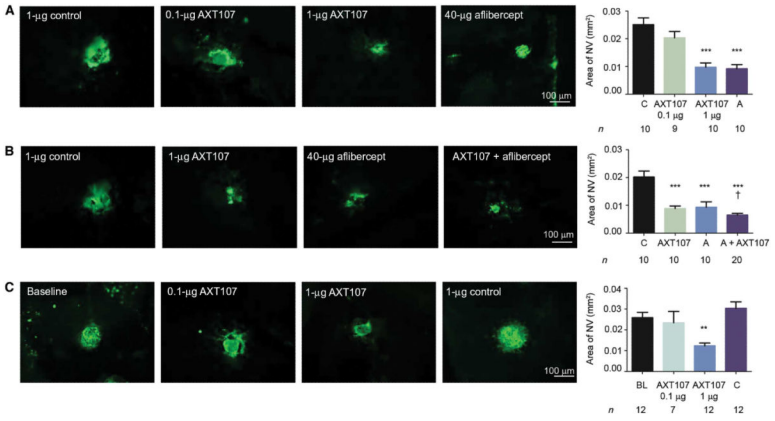

Fig. 1. The collagen IV–derived mimetic peptide AXT107 causes suppression and regression of choroidal NV

(**A**) C57BL/6 mice had laser-induced rupture of Bruch's membrane at three locations in one eye followed by an intraocular injection of 0.1 or 1 μg of AXT107, 1 μg of scrambled control peptide, or 40 μg of aflibercept. After 14 days, mice were euthanized, and retinas were dissected, stained with *Griffonia simplicifolia* lectin (GSA), and flat-mounted. (**B**) Eyes injected with 1 μg of AXT107 and 40 μg of aflibercept had significantly greater reduction in area of choroidal NV than either alone. (**C**) C57BL/6 mice ($n = 43$) had laser-induced rupture of Bruch's membrane at three locations in one eye, and after 7 days, 12 mice were euthanized and the baseline mean area of choroidal NV was measured. The remaining mice received an injection of 0.1 or 1 μg of AXT107 or 1 μg of control peptide, and 7 days after injection, the mice were euthanized and the area of choroidal NV was measured. C, control; A, aflibercept; BL, baseline. Bars represent mean (± SEM). $^{***}P < 0.001$ for difference from control, $^{**}P < 0.01$ for difference from baseline, $^{\dagger}P < 0.05$ for difference from AXT107 or aflibercept by analysis of variance (ANOVA) with Bonferroni correction for multiple comparisons.

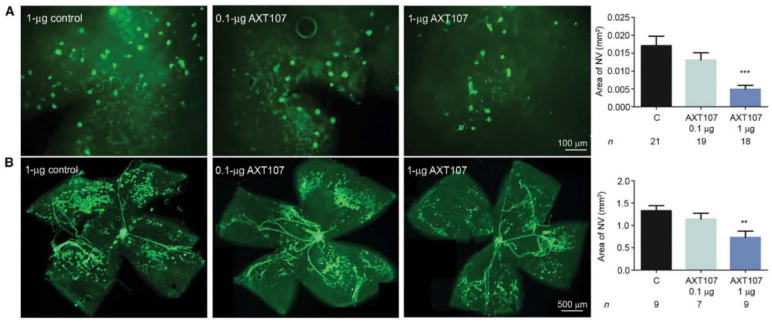

Fig. 2. The collagen IV–derived peptide AXT107 suppresses VEGF-induced subretinal NV and ischemia-induced retinal NV

(**A**) At P14, *rho/VEGF* transgenic mice in which the rhodopsin promoter drives expression of VEGF in photoreceptors were given an intraocular injection of 0.1 or 1 μg of AXT107 or 1 μg of control peptide. At P21, the area of subretinal NV on GSA-stained retinal flat mounts oriented with photoreceptor side up was measured. (**B**) At P12, C57BL/6 mice with OIR were given an intraocular injection of 0.1 or 1 μg of AXT107 or 1 μg of control peptide. At P17, retinas were incubated for 40 min with GSA, which selectively stains NV (patches of dark green) and hyaloid vessels (snake-like structures) and does not stain preexisting retinal vessels. Bars represent mean (± SEM). $^{**}P < 0.01$, $^{***}P < 0.001$ for difference from control by ANOVA with Bonferroni correction for multiple comparisons.

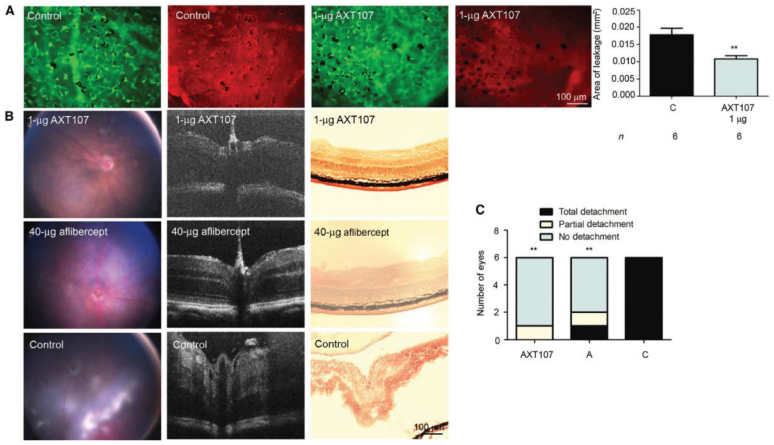

Fig. 3. AXT107 reduces leakage from subretinal NV in rho/VEGF mice and decreases exudative retinal detachment in Tet/opsin/VEGF mice

(**A**) At P20, rho/VEGF mice were injected intraocularly with 1 μg of AXT107 or vehicle (control) and, at P21, were perfused through the left ventricle with phosphate-buffered saline (PBS), and retinas were stained with GSA (green) and immunostained for albumin (red). Bars represent mean (± SEM). $^{**}P < 0.01$ by unpaired *t* test. (**B**) Male Tet/opsin/VEGF double-transgenic mice with doxycycline-inducible expression of VEGF in photoreceptors were given an intraocular injection of 1 μg of AXT107, 40 μg of aflibercept, or vehicle in one eye ($n = 6$ in each group) and then given doxycycline (2 mg/ml) in drinking water. After 4 days, fundus photographs (left column) and optical coherence tomography (OCT) images (second column) were taken, and then mice were euthanized and ocular frozen sections were stained with hematoxylin (right column). (**C**) Compared with controls, the incidence of detachment was significantly less in AXT107- or aflibercept-injected eyes. $^{**}P < 0.015$ by Fisher's exact test. C, control; A, aflibercept.

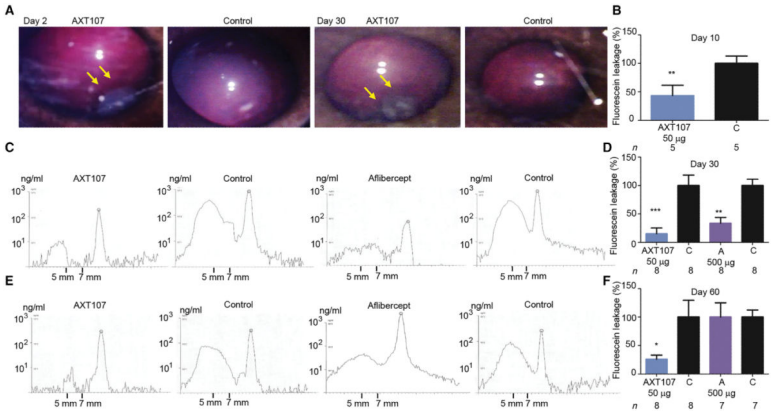

Fig. 4. Intraocular injection of AXT107 reduces VEGF-induced leakage for at least 2 months in rabbit eyes

(**A**) Fundus photography 2 days after intraocular injection of 50 μg of AXT107 in Dutch Belted rabbits. The vitreous was clear with no evidence of inflammation, and a gel-like depot was seen in the inferior vitreous at the site of injection (left panel, arrows) and was still seen in the same location 30 days after injection (third panel, arrows). (**B**) VEGF (10 μg) was injected in both eyes3 days after injection of 50 μg of AXT107 in one eye, and after 7 days, VFP showed fluorescein leakage reduced by 60% in AXT107-injected eyes (***P* = 0.007 by unpaired *t* test). (**C**) In another group of rabbits, 10 μg of VEGF was injected in both eyes 23 days after injection of 50 μg of AXT107 or 500 μg of aflibercept in one eye, and at 30 days, VFP scans showed low levels of sodium fluorescein in the mid-vitreous between 5 and 7 mm in front of the retina in AXT107- or aflibercept-injected eyes compared with fellow control eyes. (**D**) Quantification of VFP images in (C) showed that leakage was reduced by 86% in AXT107-injected eyes and 69% in aflibercept-injected eyes (***P* < 0.01, ****P* < 0.001 by unpaired t test from corresponding controls). (**E**) The rabbits from (D) were rescanned without injection of sodium fluorescein on day 43, and vitreous fluorescence was back to baseline levels. On day 53, 10 μg of VEGF was injected into each eye, and on day 60, VFP scans showed low levels of fluorescein in the mid-vitreous of AXT107-injected eyes and higher levels in control and aflibercept-injected eyes. (**F**) Quantification of VFP images in (E) showed that leakage was reduced by 70% in AXT107-injected eyes compared to corresponding controls (**P* = 0.035 by unpaired *t* test) but not in aflibercept-injected eyes (A). Bars represent mean (± SEM).

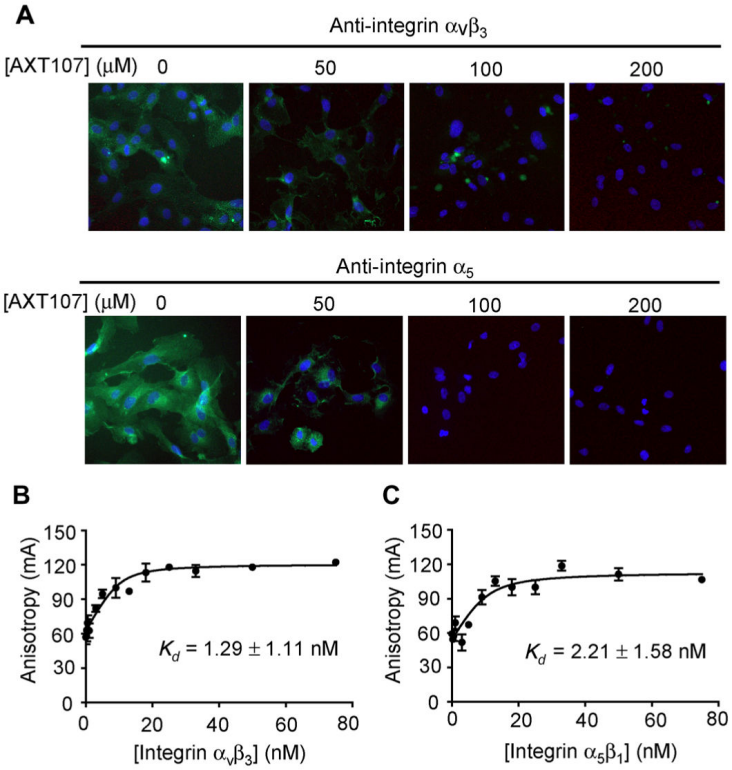

Fig. 5. AXT107 binds integrins $\alpha_v\beta_3$ and $\alpha_5\beta_1$

(**A**) Incubation of AXT107 with HRECs reduced binding of anti–integrin $\alpha_v\beta_3$ (top) or anti–integrin α_5 antibodies (bottom). Anti-integrin antibodies were visualized by immunohistochemistry with fluorescein isothiocyanate (FITC)–labeled secondary antibodies (green), and nuclei were stained with 4′,6-diamidino-2-phenylindole (blue). (**B** and **C**) Change in anisotropy of 5-FAM–labeled AXT107 (10 nM) at various concentrations of integrin $\alpha_v\beta_3$ (B) or $\alpha_5\beta_1$ (C). K_d values were determined by fitting data to a ligand-dependent, quadratic equation of anisotropy and shown as $K_d \pm$ SD.

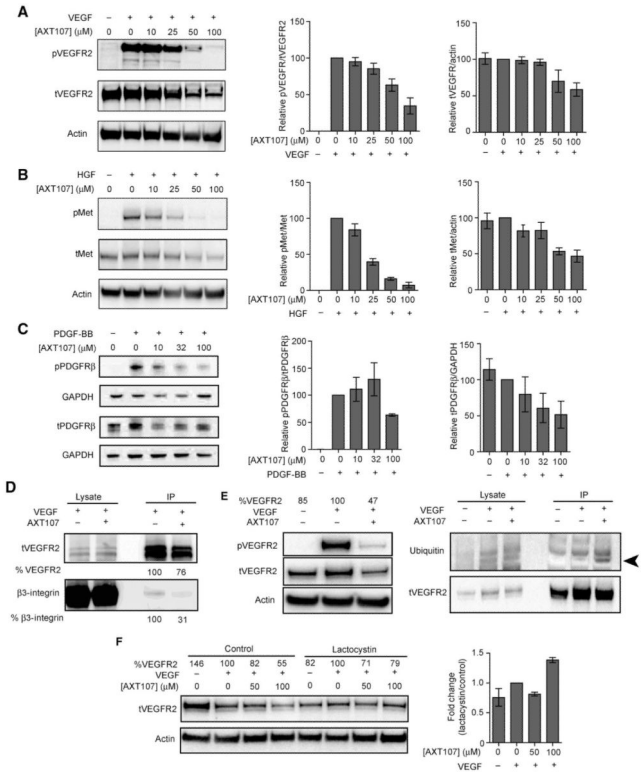

Fig. 6. AXT107 inhibits VEGF-, HGF-, and PDGF-BB–stimulated phosphorylation of VEGFR2, c-Met, and PDGFRb receptors

(**A**) HRECs were stimulated with VEGF (25 ng/ml) for 5 min in the presence of increasing concentrations of AXT107 at 0, 10, 25, 50, and 100 μM peptide. The lysates were then immunoblotted with phosphorylated VEGFR2 (Y1175) (pVEGFR2) and anti-VEGFR2 (tVEGFR2) antibody (left). The blots were probed with anti-actin antibody as a loading control. Images were quantified by densitometry to determine the amount of total VEGFR2 normalized by actin (middle) and the ratio of phospho-VEGFR to total VEGFR2 (right) at each peptide concentration relative to the VEGF-treated, 0 μM AXT107 sample; mean ± SEM, $n = 3$. (**B**) Same as in (A), except that cells were stimulated with HGF (50 ng/ml) for 15 min and probed with anti–phosphorylated c-Met (Y1234/1235) (pMet) and anti–c-Met antibodies [total c-Met protein (tMet)]; mean ± SEM, $n = 3$. (**C**) 3T3 fibroblasts were stimulated with PDGF-BB (50 ng/ml) for 10 min after a 90-min treatment with 0, 10, 32, or 100 μM AXT107. Lysates were probed with anti–phosphorylated PDGFRβ (Y751) (pPDGFRβ) and anti-PDGFRβ antibodies (tPDGFRβ) and anti–glyceraldehyde phosphate dehydrogenase (GAPDH) as a loading control; mean ± SEM, $n = 3$. (**D**) AXT107 at 60 μM dissociates β_3 integrin from the VEGFR2-β_3 complex. VEGFR2 was immunoprecipitated (IP) from VEGF-stimulated HRECs in the presence and absence of AXT107 after cross-linking and immunoblotted with anti-β_3 integrin and anti-VEGFR2 antibody. Images were quantified by densitometry to determine the amount of total VEGFR2 immunoprecipitated in the presence and absence of AXT107 in blots probed with anti-VEGFR2. The same was done for β_3 in blots probed with anti-β_3. The values for VEGFR2 and β_3 in HREC samples stimulated with VEGF in the absence of AXT107 were considered 100%, and the values for VEGFR2 and β_3 in HREC samples stimulated with VEGF in the presence of AXT107 were

expressed as a percent of those values. (**E**) AXT107 at 60 μM promotes ubiquitination of VEGFR2. HRECs were untreated, treated with VEGF, or treated with VEGF and 60 μM AXT107. There was a 53% reduction in VEGFR2 protein in cells treated with AXT107 and VEGF compared with those treated with VEGF alone (right panel). To compensate, twice as much lysate from cells treated with both AXT107 and VEGF than lysate from cells treated with VEGF alone was immunoprecipitated with anti-VEGFR2 and immunoblotted with anti-ubiquitin antibody FK2 and anti-VEGFR2 antibody. Ubiquitinated VEGFR2 band (arrowhead) is detected in immunoprecipitates from VEGF-stimulated HRECs incubated with 60 μM AXT107 and not in immunoprecipitates from VEGF-stimulated HRECs in the absence of peptide or nonstimulated cells. (**F**) Proteasomal inhibition restored VEGFR2 levels. (Left) Representative image of Western blot showing changes in total VEGFR2 in lysates from cells treated with varying concentrations of AXT107 in the presence or absence of 5 μM lactacystin with actin as a loading control. % VEGFR2 values indicate densitometric analysis of tVEGFR2 bands normalized to actin and presented as percentages relative to VEGF-only samples for the corresponding lactacystin treatment. (Right) Change in the relative total VEGFR2 in lactacystin-treated cells compared to control cells; mean ± SEM, $n = 3$.